

Activated Ezrin Promotes Cell Migration through Recruitment of the GEF Dbl to Lipid Rafts and Preferential Downstream Activation of Cdc42[□]

Soren Prag,^{*†‡§} Maddy Parsons,^{†‡} Melanie D. Keppler,^{*†} Simon M. Ameer-Beg,^{*†} Paul Barber,^{||} James Hunt,^{†¶} Andrew J. Beavil,^{†¶} Rosy Calvert,^{†¶} Monique Arpin,[#] Borivoj Vojnovic,^{||} and Tony Ng^{*†}

^{*}Richard Dumbleby Department of Cancer Research, [†]Randall Division of Cell and Molecular Biophysics, and [¶]Division of Asthma, Allergy, and Lung Biology, King's College London, Guy's Medical School Campus, London SE1 1UL, United Kingdom; ^{||}Gray Cancer Institute, Oxford University, Mount Vernon Hospital, Northwood, Middlesex, HA6 2JR, United Kingdom; and [#]Laboratoire de Morphogenese et Signalisation Cellulaires, Institut Curie, 75248 Paris Cedex 05, France

Submitted November 21, 2006; Revised May 18, 2007; Accepted May 23, 2007
Monitoring Editor: Paul Forscher

Establishment of polarized cell morphology is a critical factor for migration and requires precise spatial and temporal activation of the Rho GTPases. Here, we describe a novel role of the actin-binding ezrin/radixin/moesin (ERM)-protein ezrin to be involved in recruiting Cdc42, but not Rac1, to lipid raft microdomains, as well as the subsequent activation of this Rho GTPase and the downstream effector p21-activated kinase (PAK)1, as shown by fluorescence lifetime imaging microscopy. The establishment of a leading plasma membrane and the polarized morphology necessary for random migration are also dependent on ERM function and Cdc42 in motile breast carcinoma cells. Mechanistically, we show that the recruitment of the ERM-interacting Rho/Cdc42-specific guanine nucleotide exchange factor Dbl to the plasma membrane and to lipid raft microdomains requires the phosphorylated, active conformer of ezrin, which serves to tether the plasma membrane or its subdomains to the cytoskeleton. Together these data suggest a mechanism whereby precise spatial guanine nucleotide exchange of Cdc42 by Dbl is dependent on functional ERM proteins and is important for directional cell migration.

INTRODUCTION

The ezrin/radixin/moesin (ERM) family of proteins are involved in regulation of cellular morphology and migration, and a direct interaction with actin filaments provides a regulatory link between the cytoskeleton and the cell membrane (Crepaldi *et al.*, 1997; Lamb *et al.*, 1997; Bretscher *et al.*, 2002). Activation of ERM proteins occurs by conformational changes triggered by binding of phosphatidylinositol 4,5-bisphosphate (PIP₂) to the FERM (band 4.1, ERM) domain in the NH₂-

terminal region, termed the NH₂-terminal ERM-associated domain (N-ERMAD) and phosphorylation of a conserved threonine residue (ezrin-T567, radixin-T564, moesin-T558) in the COOH-terminal domain, termed the COOH-terminal ERM-associated domain (C-ERMAD; Pietromonaco *et al.*, 1998; Barret *et al.*, 2000; Ng *et al.*, 2001; Fievet *et al.*, 2004). This sequence of molecular events releases the intramolecular interaction between the N- and C-termini. Several kinases, including myotonic dystrophy kinase-related Cdc42-binding kinase Several kinases, including myotonic dystrophy kinase-related Cdc42-binding kinase (Nakamura *et al.*, 2000), protein kinase C α (Ng *et al.*, 2001), and Nck-interacting kinase (Baumgartner *et al.*, 2006) have been shown to phosphorylate the conserved C-terminal threonine in ERM proteins. This second activation step of phosphorylation may restrict actin tethering by ERM proteins to specialized membrane domains, such as the protruding cell membranes, by locally unmasking the binding site for actin filaments in C-ERMAD. These changes in the ERM proteins also expose binding sites in N-ERMAD for plasma membrane receptors and scaffold proteins including CD44, CD43, ICAMs, and EBP50 (Reczek *et al.*, 1997; Yonemura *et al.*, 1998; Legg *et al.*, 2002). It is not clear however whether the affinity or availability of binding sites of N-ERMAD for these protein partners are affected by C-ERMAD binding (Chambers and Bretscher, 2005). Establishment of polarity is essential for directed cell motility and requires localization of sensory and signaling molecules to the leading edge of a migrating cell. One such family of molecules are the small Rho GTPases, in partic-

This article was published online ahead of print in *MBC in Press* (<http://www.molbiolcell.org/cgi/doi/10.1091/mbc.E06-11-1031>) on May 30, 2007.

[□] The online version of this article contains supplemental material at *MBC Online* (<http://www.molbiolcell.org>).

[†] These authors contributed equally to this work.

[§] Present address: Instituto de Medicina Molecular, Faculdade de Medicina de Lisboa, Portugal.

Address correspondence to: Soren Prag (sprag@fm.ul.pt) or Tony Ng (tony.ng@kcl.ac.uk).

Abbreviations used: C-ERMAD, COOH-terminal ERM-associated domain; CTxB, cholera toxin subunit B; ERM, ezrin/radixin/moesin; FERM, band 4.1, ezrin, radixin, moesin; FLIM, fluorescent lifetime imaging measurements; FRET, Förster resonance energy transfer; GEF, guanine nucleotide exchange factor; N-ERMAD, NH₂-terminal ERM-associated domain.

ular Cdc42 and Rac (Etienne-Manneville and Hall, 2002; Ridley *et al.*, 2003). The activation of Cdc42 and Rac1 is essential for protrusion and formation of filopodia and lamellipodia in eukaryotic cells, via the reorganization of the actin cytoskeleton, which leads to changes in cell morphology and migration (Kozma *et al.*, 1995; Nobes and Hall, 1995; Leung *et al.*, 1998). Cdc42 is found in its active GTP-bound state at the leading edge of migrating cells (Itoh *et al.*, 2002), and inactivation of Cdc42 inhibits cell polarization and lamellipodial protrusions (Nobes and Hall, 1999). Recently it has been shown that the GTP-bound Rac1 localizes preferentially to the low density, cholesterol- and caveolin-enriched membranes in human fibroblasts (del Pozo *et al.*, 2004). Furthermore, in cells detached from the extracellular matrix, endogenous Rac1 is recruited to cholera toxin subunit B (CTxB)-clustered lipid raft microdomains. This enables the sustained activation of p21-activated kinase (PAK) 1, a downstream effector of Rac and Cdc42 (del Pozo *et al.*, 2004). The lipid raft microdomain has therefore been proposed as a preferential membrane site for active GTPases, but the mechanisms by which these molecules are recruited to and more importantly, activated at these specific microdomains, are not well understood. In addition to membrane targeting, the activity of Rho GTPases is regulated by guanine nucleotide exchange factors (GEFs), promoting the exchange of GDP to GTP, and GTPase-activating proteins (GAPs), which stimulate the intrinsic GTPase activity upon binding to their respective GTPases. Currently there is limited information on the functional link between ezrin and Rho GTPase activation. Both the C-terminal threonine phosphorylated form of ERM and the phosphomimetic (T567D) ezrin mutant have been found to coprecipitate with Dbl in lymphocytes, in a complex that exhibits GEF activity toward RhoA *in vitro* (Lee *et al.*, 2004). The physiological effect of expressing T567D ezrin in these cells is an enhancement of uropod formation. On the basis of structure-function analyses performed on the N-ERMAD, we have designed novel molecular tools that allow us to segregate the C-ERMAD-binding function of N-ERMAD from the latter's ability to associate with other protein ligands. Our data demonstrate that a mutant N-ERMAD of ezrin (which has a much reduced affinity to C-ERMAD) retains the ability to block cell migration as well as the lipid raft localization and activation of Cdc42, but not Rac1. Furthermore, we demonstrate that the conformational activation (phosphorylation) of ERM proteins is involved in the recruitment of the Cdc42/Rho-specific GEF Dbl to these microdomains, which acts as a potential mechanism for the spatial regulation of Cdc42 activity.

MATERIALS AND METHODS

Cell Culture and Transfection

Human breast carcinoma cells (MDA-MB-231) and human embryonic kidney (HEK)-293T cells were cultured in DMEM containing 10% fetal calf serum at 37°C, in a 5% CO₂ atmosphere. Cells were transfected using Fugene6 (Boehringer Mannheim, Indianapolis, IN) or calcium phosphate (Invitrogen, Carlsbad, CA) according to the protocol provided by the manufacturer. For Cdc42 small interfering RNA (siRNA), the 21-mer double-strand (dsRNA) sequences used were Cdc42-1: AAGTGGGTGCCTGAGATAACT, or Cdc42-2: AAAGACTCCTTCTTGCTGT, or Nonsilencing control RNA interference (RNAi; Qiagen, Chatsworth, CA), and cells were transfected with 20 nM RNAi using HiPerfect (Qiagen) according to the protocol provided by the manufacturer.

Plasmid Constructs

cDNA containing VSV G-tagged full-length ezrin, ezrin(T567A), ezrin(T567D), and N-ERMAD were described previously (Algrain *et al.*, 1993). cDNAs containing GST-ezrin, GST-N-ERMAD, and GST-C-ERMAD were described previously (Andreoli *et al.*, 1994). E244K point mutation was generated using QuikChange Site-Directed Mutagenesis Kit (Stratagene, La Jolla, CA). The mRFP1 constructs were prepared by standard PCR amplification of full-length ezrin using 5'-CGTCGTAAGCTTAAAATGCCGAAACCA-3' and

5'-CGACGAATTCACAGGGCCTCGAA-3' for full-length ezrin-mRFP1, and 5'-CGTCGTAAGCTTAAAATGCCGAAACCA-3' and 5'-CGACGAATTCCTACTGGCCTTCAT-3' for N-ERMAD-mRFP1. PCR products were cloned into pcDNA3.1-mRFP1 construct. GST-N-ERMAD(E244K) and N-ERMAD(E244K)-mRFP1 were generated as described above, using GST-N-ERMAD and N-ERMAD-mRFP1 as template. GST-Dbl(DH/PH) was subcloned into pGEX-KG from pRK5-myc-Dbl using BamHI. The PAK1-green fluorescent protein (GFP) construct was previously described (Parsons *et al.*, 2005). Onco-Dbl (pRK5-myc-Dbl) and FGD1 (pRK5-myc-FGD1) were generous gifts from Professor Alan Hall (MRC Laboratory for Molecular Cell Biology and Cell Biology Unit, London, United Kingdom). HA-Tiam1 (C1199) was a generous gift from Dr. John Collard (The Netherlands Cancer Institute, Amsterdam, The Netherlands). HA-p190RhoGEF was a generous gift from Dr. Wouter Moolenaar (National Cancer Institute), GST-RhoGDI was a generous gift from Dr. Alexis Gautreau (Institut Curie, Paris, France), Wt-Cdc42-GFP and V12Cdc42-GFP were provided by Dr. James Monypenny (Cancer Research UK London Research Institute, London). Cdc42-myc and N17Cdc42-myc was a generous gift from Dr. Julian Downward (Cancer Research UK London Research Institute).

Antibodies and Direct Conjugation to Fluorophores

Anti-VSVG and anti-myc (clone 9E10) monoclonal antibodies were generated at Cancer Research UK. The rabbit polyclonal anti-C-PERM antibody was obtained from Cell Signaling Technology (Beverly, MA). Rabbit polyclonal Dbl antibody (sc-89) was purchased from Santa Cruz Biotechnology (Santa Cruz, CA). Mouse mAb against Rac1 (23A8) was purchased from Upstate Biotechnology (Lake Placid, NY), and mouse mAb against Cdc42 was purchased from Chemicon International (Temecula, CA; MAB3707). Mouse mAb against ezrin was generated from recombinant full-length ezrin (2H3; Parsons and Ng, unpublished data). For Förster resonance energy transfer (FRET) measurement, direct conjugation of IgG to the fluorophores Cy3 (Amersham Life Science, Piscataway, NJ) was performed as described previously (Parsons and Ng, 2002).

Alexa Fluor-conjugated phalloidin was purchased from Molecular Probes (Eugene, OR).

Immunocytochemical Staining and Confocal Microscopy

Immunocytochemical stainings were performed as described elsewhere (Parsons and Ng, 2002). Images were acquired on a confocal laser scanning microscope (model LSM 510 Meta, Carl Zeiss, Thornwood, NY) using a 63×/1.4Plan-Apochromat oil immersion objective. Each image represents a single section in the Z-series, taken across the depth of the cell at 0.2- μ m intervals.

Raft Clustering by CTxB-coated Beads

Clustering of raft-associated ganglioside GM1 by CTxB beads was performed as previously described (del Pozo *et al.*, 2004). Briefly, cells were plated onto coverslips and left to adhere and spread for 24 h. For exogenous expression experiments, cells were microinjected with plasmids as indicated and allowed to express for 6 h. A solution of polystyrene 3- μ m beads coated overnight at 4°C with 10 μ g/ml CTxB (Calbiochem, La Jolla, CA) were added to cells for 20 min at 37°C. Cells were fixed in 4% paraformaldehyde and stained with antibodies as indicated and imaged on confocal microscope as described.

Protein Purification and In Vitro Pulldown Assays

Glutathione S-transferase (GST)-fusion proteins were expressed in Top10 *Escherichia coli* (Invitrogen) and affinity-purified using GST-agarose (Sigma, St. Louis, MO). C-ERMAD, RhoGDI, and Dbl(PH/DH) proteins were purified as GST-fusion proteins and enzymatically digested by thrombin to remove the GST according to protocols provided by the manufacturer (Amersham, Little Chalfont, Buckinghamshire, United Kingdom). Pulldown assays were performed by tumbling purified C-ERMAD, RhoGDI or Dbl(PH/DH) with GST, GST-N-ERMAD, or GST-N-ERMAD(E244K) bound to agarose beads. After extensive washes in lysis buffer, samples were resuspended in Laemmli sample buffer containing SDS. Cdc42 and Rac1 GTPase activity assays were performed as previously described (Parsons *et al.*, 2005) using GST-PBD-PAK1. Rho GTPase activity assays were performed using GST-Rhotekin agarose (Upstate).

Protein Transduction using Chariot

Cells (grown on 3-cm tissue culture dishes to ~70% confluency) were transduced with purified proteins, as indicated, using Chariot (Active Motif Europe, Rixensart, Belgium) according to manufacturer's instructions. Briefly, 2 μ g of proteins were diluted in 100 μ l PBS and then added to 100 μ l H₂O containing 6 μ l of the Chariot reagent. The Chariot:protein mix was left to stand in room temperature for 30 min before adding to cells in 400 μ l serum-free medium. After 1 h of incubation at 37°C, 1 ml of serum-containing medium was added to each dish. Cells were used for various assays (see Figures 2, 3, and 10) after a further 30-min incubation. For ensuring equal transduction efficiencies, in parallel experiments, recombinant full-length (FL) ezrin (0.059 mg/ml), N-ERMAD (0.015 mg/ml), or N-ERMAD(E244K) (0.02 mg/ml) that were obtained from GST-fusion proteins after thrombin cleavage

were labeled with Cy3 (Amersham Life Science) before being transduced into cells.

Biacore Surface Plasmon Resonance Experiments

Immobilization of anti-GST on the CM5 sensor surface was performed according to the protocol provided by the manufacturer (GST Capture Kit, Biacore International, Switzerland) to a total of 4500 responsive units (RU) on a Biacore 3000 instrument (Biacore International, part of GE Healthcare UK Ltd., Little Chalfont, Buckinghamshire, United Kingdom). GST or GST-fusion proteins were captured on individual flowcells from soluble fraction of crude extracts from *E. coli* expressing the indicated fusion proteins after diluted 10 times in HBS buffer (10 mM HEPES, pH 7.4, 150 mM NaCl, 3 mM EDTA, 0.005% P20, 1 mM phenylmethylsulfonyl fluoride) injected at flow rate of 5 μ l/min for 200 s, generating a consistent 500 RU GST-fusion protein surface. After injection, surfaces were washed with HBS buffer for 600 s with a minimal baseline drift of 2–5 RU/min, before injection of purified C-ERMAD, RhoGDI, or Dbl(PH/DH), diluted in HBS to concentrations ranging from 5 nM to 2 μ M, with a flow rate of 30 μ l/min. Each surface was regenerated by two pulse-injections of 0.5% SDS BIA-desorb solution 1 (Biacore). Apparent $K_{d,s}$ were calculated by global fit analysis or steady state affinity employing BIAevaluation 3.0 software after traces were baseline-corrected by subtraction of parallel control surface capturing GST alone.

Transwell Chamber Migration Analysis

Purified ezrin, N-ERMAD or N-ERMAD(E244K) proteins were transduced into MDA-MB-231 cells using Chariot according to the protocols provided by the manufacturer. After 90 min at 37°C, cells were trypsinized and replated into six-well (24-mm insert) transwell plates (Costar, Cambridge, MA) at a concentration of 5×10^5 cells/well in DMEM containing 1% fetal calf serum (FCS). The bottom well in each case contained DMEM supplemented with 1% FCS and 1 μ M phorbol 12,13-dibutyrate (PDBu; Sigma), except for control wells, which contained 1% FCS alone. Cells were incubated for 8 h at 37°C, trypsinized separately from each top and bottom well, centrifuged at 1000 rpm, and fixed in 4% paraformaldehyde. Total numbers of cells in each chamber were counted using a CASY-1 cell counter (Sharfe System, GmbH, Reutlingen, Germany) and migration was calculated as the percentage of cells in bottom chamber out of total number of cells, and an average from three individual wells per treatment was calculated in each experiment. Transmigration were normalized against control cells set at 100%.

Time-Lapse Analysis and Cell Tracking

Random migration of cells was assessed using time-lapse microscopy. Briefly, MDA-MB-231 cells were plated in 12-well dishes (Nunc, Naperville, IL) 24 h before recording in thermostatically controlled chamber (Solent Scientific Limited, Segensworth, United Kingdom) surrounding a Zeiss AxioVert 100 microscope using a 10 \times phase-contrast objective and IQ software (Andor, Belfast, Northern Ireland). Images were captured using a Senciam QE digital CCD camera (Cooke, Auburn Hills, MI). Frames were acquired every 5 min over a total period of 2 h. Analysis of speed was performed by manually tracking cells within each field over the sequence of time-lapse digital images (Motion Analysis Software, Andor, UK). The resultant cell tracks were analyzed using Mathematica software and comparisons between different groups of cell mean speed tracks were statistically assessed by analysis of variants (ANOVA).

FRET Determination by Multiphoton Fluorescence Lifetime Imaging Microscopy Measurements

Time-domain fluorescence lifetime imaging microscopy (FLIM) was performed with a multiphoton microscope system, comprising a solid-state-pumped (8 W Verdi, Coherent, Palo Alto, CA), femtosecond self-mode-locked Ti:Sapphire (Mira, Coherent) laser system, an in-house developed scan-head and an inverted microscope (Nikon TE2000E, Melville, NY) as described previously (Peter *et al.*, 2005). The presence/absence of FRET is determined by fitting of the experimental data to a single exponential decay. Significant reduction in the measured lifetime indicates FRET.

Immunoprecipitation and Western Blotting

MDA-MB-231 cells were transfected and/or treated as described in the text. Cells were lysed in modified RIPA buffer (1% (wt/vol) *n*-octyl- β -glucopyranoside, instead of NP-40) for 30 min at 4°C. Indicated antibodies were bound to protein A/G agarose beads (Autogen Bioclear UK Ltd., Calne, Wiltshire, United Kingdom), and the resulting bead solution was incubated with cell lysates overnight at 4°C. A sample of the “unbound” fraction was removed for analysis, and the beads were washed extensively in lysis buffer after binding. The precipitated proteins were denatured in sample buffer, separated on SDS-PAGE under reducing conditions, and transferred electrophoretically to nitrocellulose membrane (Amersham). Blots were probed with antibodies as specified.

RESULTS

Mutation of Glutamic Acid 244 in the N-ERMAD of Ezrin Decreases Its Binding to the C-ERMAD and Enhances Its Dominant Inhibition of Cell Migration

A number of studies have utilized the N-ERMAD of ERM proteins as dominant inhibitory constructs and demonstrated that the introduction of this domain alone can alter the function of endogenous ERM proteins, but the molecular

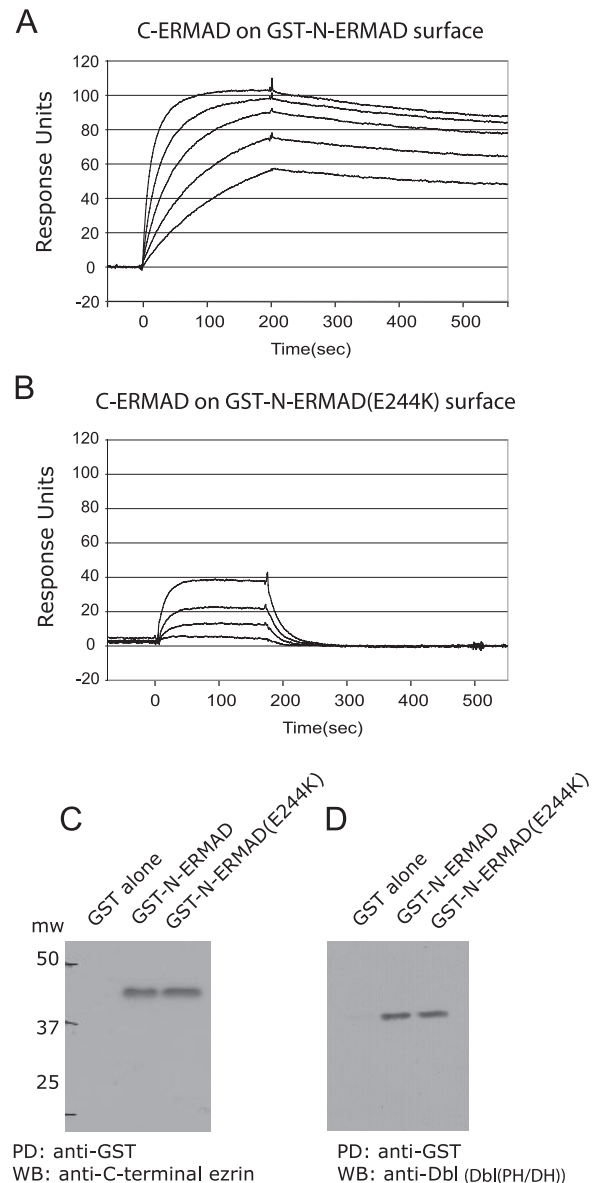


Figure 1. Mutation of glutamic acid 244 in the N-ERMAD of ezrin decreases its association with the C-ERMAD. (A and B) Anti-GST was immobilized to a CM5 sensor to 4500 RU before capturing GST-N-ERMAD (A) or GST-N-ERMAD(E244K) (B) from crude extracts from transformed *E. coli*. Interaction with purified C-ERMAD (1.25–200 nM), was monitored at 30 μ l/min in HBS buffer. Traces were baseline-corrected by subtraction of data collected from control surface capturing GST alone. The binding of purified C-ERMAD (C) or Dbl(PH/DH) (D) to GST, GST-N-ERMAD, or GST-N-ERMAD(E244K) bound to agarose beads was assessed in vitro by the GST pull-down assay as described in *Materials and Methods*. Immunoblotting was performed with an anti-ezrin C-terminus mAb (2H3) (C) or an anti-Dbl antibody (D). One representative of three independent experiments is shown.

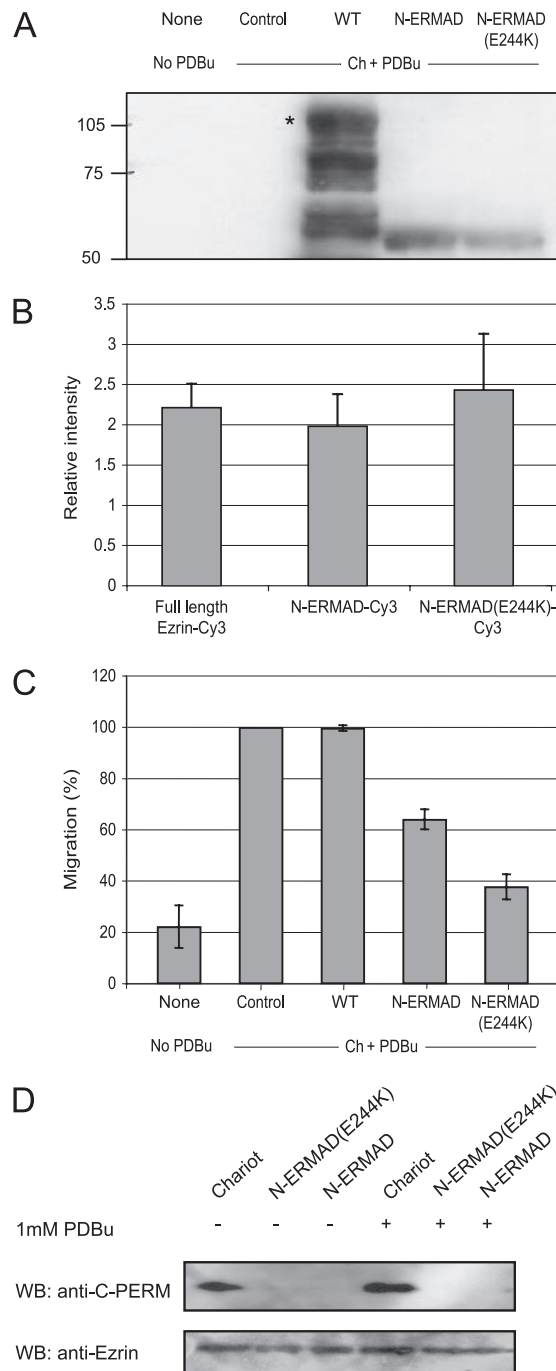


Figure 2. N-ERMAD and N-ERMAD(E244K) inhibit migration of MDA-MB-231 cells. (A) Transduction efficiency of GST-tagged full-length ezrin, N-ERMAD, and N-ERMAD(E244K). Recombinant proteins, 2 μ g, were transduced into MDA-MB-231 cells using Chariot. Asterisk denotes the expected molecular weight species for the tagged, intact full-length ezrin. Control = Chariot alone mock transduction. (B) Average fluorescent intensity (per field of view) of Cy3-conjugated full-length ezrin, N-ERMAD, or N-ERMAD(E244K) introduced into MDA-MB-231 cells by Chariot-mediated transduction. Fluorescent intensity values were quantified from confocal images, and means were calculated from six images (at least 15 cell images in each field of view). (C) The dominant inhibitory effects of N-ERMAD and N-ERMAD(E244K) on PKC-mediated cell migration were evaluated by Transwell migration of MDA-MB-231 cells. Full-length ezrin, N-ERMAD, and N-ERMAD(E244K) were purified and transduced into MDA-MB-231 cells using Chariot, and the cells

mechanism whereby the N-ERMAD achieves dominant inhibition is hitherto poorly understood (Martin *et al.*, 1995; Crepaldi *et al.*, 1997; Amieva *et al.*, 1999). The N-ERMAD can either bind to receptors or scaffolding proteins at the plasma membrane, and thus abrogate binding of endogenous ERM proteins, or interacts directly with the C-ERMAD and thus altering the actin-binding capacities of endogenous ERM proteins. To separate the C-ERMAD-binding function of N-ERMAD from the latter's ability to associate with other protein ligands, we chose to generate a single mutation Glu244 to Lys (E244K) in the ezrin N-ERMAD, which is intended to modulate the hydrogen bonds between Glu244 and Arg570 in the helix D of the C-ERMAD, hence disrupting the N-ERMAD/C-ERMAD interface (Hamada *et al.*, 2000; Pearson *et al.*, 2000). Using BIAcore surface plasmon resonance technology, we monitored the interaction between C-ERMAD and N-ERMAD. For this, we immobilized monoclonal anti-GST antibodies and by captured GST-N-ERMAD on the chip, we were able to assess the interaction between GST-N-ERMAD and C-ERMAD and obtain an estimated K_d of 1.5×10^{-9} M for the N-ERMAD:C-ERMAD association (Figure 1A). As shown in Figure 1B, the N-ERMAD(E244K) showed a 400-fold decrease in the binding affinity toward C-ERMAD with a K_d of 6×10^{-7} M compared with that of the wild-type (WT) N-ERMAD (K_d of 1.5×10^{-9} M). We attempted to ascertain, using similar methodologies, the binding affinities of GST-N-ERMAD and N-ERMAD(E244K) toward purified Dbl(DH/PH) and Rho-GDI proteins. Unfortunately, the nonspecific binding of Dbl(DH/PH) to parallel control surface capturing GST alone was too high for us to estimate the specific binding of Dbl(DH/PH) to the N-ERMADs. No binding of N-ERMAD(E244K) or (WT) N-ERMAD to purified Rho-GDI protein (up to 1 μ M) was seen by BIAcore analyses under similar experimental conditions (data not shown).

In addition, we analyzed the binding of the WT versus mutant GST-N-ERMAD (immobilized on beads) to purified C-ERMAD and Dbl protein preparations using an independent approach, namely GST pulldown followed by Western blot analysis. Immunodetection of C-ERMAD was achieved by in-house mAb 2H3 that specifically recognizes the C-terminus of ezrin (Parsons and Ng, unpublished data). Despite the BIAcore analyses, which reproducibly showed the N-ERMAD(E244K) to have a substantially reduced affinity (K_d of 6×10^{-7} M; in comparison to the binding of [WT] N-ERMAD to purified C-ERMAD; K_d of 1.5×10^{-9} M), it was able to capture a similar amount of C-ERMAD after a prolonged incubation (overnight at 4°C), i.e., when the binding reaction has reached the equilibrium (Figure 1D). Similarly, at equilibrium, the *in vitro* binding of purified Dbl(PH/DH) to GST-N-ERMAD was not significantly affected by the E244K mutation (Figure 1D). The equivalent assay for Rho-GDI binding was not successful because the anti-Rho-GDI antibody we used had a high nonspecific binding to the GST itself (data not shown).

were allowed to transmigrate for 8 h at 37°C. The total amounts of cells in the bottom and top chamber were counted and the percentages of migrated cells in the bottom chamber out of total amount of cells were calculated and normalized against control cells set at 100%. One representative of three independent experiments is shown. (D) Western blot analysis of whole cell lysates from MDA-MB-231 cells untreated, stimulated with 1 μ M PDBu for 20 min at 37°C, or transduced with purified N-ERMAD(E244K) or N-ERMAD protein using Chariot. Blots were probed with anti-C-PERM or anti-ezrin antibodies. Results showed are representative of three independent experiments.

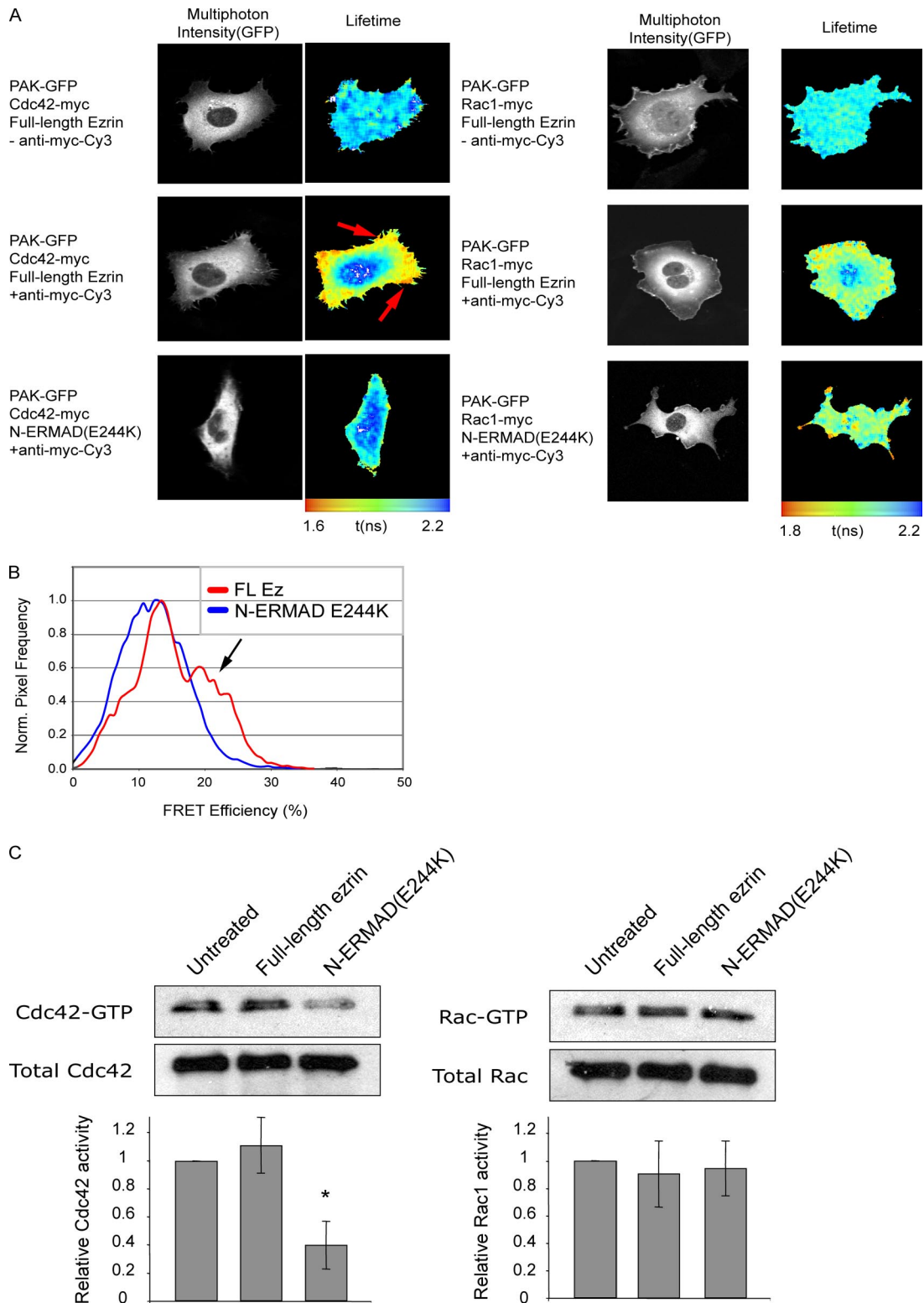


Figure 3. N-ERMAD(E244K) decreases the association between Cdc42 and the downstream effector PAK1 and specifically decreases Cdc42 activity. (A) MDA-MB-231 cells were microinjected with PAK1-GFP, myc-Cdc42, and full-length ezrin or N-ERMAD(E244K). Six hours after injection, cells were fixed with 4% PFA and mounted (–anti-myc-Cy3) or stained with Cy3-conjugated antibodies toward myc (+anti-myc-Cy3). The association between PAK-GFP and Cdc42-myc-Cy3 (left panel) and Rac1-myc-Cy3 (right panel) was evaluated by measuring the donor fluorescent lifetime (τ) of PAK-GFP by multiphoton microscopy. (B) Normalized, cumulative FRET efficiency histogram compiled from all the data sets ($n = 5$ cells) for PAK-GFP:Cdc42-myc-Cy3 in the presence of full-length ezrin or N-ERMAD(E244K). FRET efficiency = $1 - \tau_{da}/\tau_d$, where τ_{da} is the pixel-by-pixel fluorescence lifetime of the donor in the presence of the Cy3 acceptor and τ_d is the average lifetime of the donor in the absence of acceptor. Arrows indicate a pronounced enrichment of the PAK-GFP:Cdc42-myc-Cy3-interacting species in the cell protrusion structures of full-length ezrin-expressing cells. (C) Quantification of Cdc42 and Rac1 activity. Purified full-length ezrin or N-ERMAD(E244K) was transduced into MDA-MB-231 cells for 2 h.

The dominant inhibitory effect of N-ERMAD of ezrin on cell migration of several cell types has previously been described (Crepaldi *et al.*, 1997; Sahai and Marshall, 2003). We therefore tested the effect of the E244K mutation in N-ERMAD on migratory behavior of breast carcinoma cells by transducing recombinant proteins into MDA-MB-231 cells using Chariot. We measured the transduction efficiency of GST-tagged full-length ezrin, N-ERMAD, and N-ERMAD(E244K) and compared protein loading by immunoblotting. As shown in Figure 2A, GST-tagged full-length ezrin, N-ERMAD, and N-ERMAD(E244K) were transduced in similar amounts (GST-tagged full-length ezrin marked with *). Furthermore, to verify that the transduction efficiency was also equal in non-GST-tagged forms of the proteins (which were used in subsequent experiments), we transduced cells with thrombin-treated, Cy3-conjugated recombinant full-length ezrin, N-ERMAD, and N-ERMAD(E244K) and measured levels of Cy3 fluorescence in MDA-MB-231 cells after transduction. The mean fluorescent intensities (per field of view) of Cy3-conjugated full-length ezrin, N-ERMAD, and N-ERMAD(E244K) in these cells were 2.21 ± 0.31 , 1.98 ± 0.38 , and 2.43 ± 0.70 (SEM for $n = 6$ images, Figure 2B), respectively, indicating that the recombinant proteins were transduced in equal amounts. Transduction of full-length ezrin into MDA-MB-231 cells had no effect on the transmigration of cells toward the protein kinase C (PKC) activator PDBu (Ng *et al.*, 1999; Legg *et al.*, 2002) compared with cells treated with the Chariot alone (Figure 2C). Transduction of the N-ERMAD protein decreased MDA-MB-231 cell migration by 46.1%, whereas mutation of E244K in the N-ERMAD protein inhibited cell migration by 79.2% compared with the full-length ezrin (Figure 2C). This demonstrates that introduction of an E244K mutation in the N-ERMAD enhances the dominant effects of N-ERMAD as evaluated by inhibition of PKC-mediated cell migration. We also tested the effect of N-ERMAD and N-ERMAD(E244K) on the threonine phosphorylation of the C-ERMAD (C-PERM). Western blot analysis of cell lysates from untreated cells showed a basal level of C-PERM, and upon stimulating the cells with $1 \mu\text{M}$ PDBu a $44.3 \pm 10.9\%$ (SEM, $n = 3$) increase in C-PERM was observed (Figure 2D). In contrast, upon transducing purified N-ERMAD or N-ERMAD(E244K) into MDA-MB-231 cells, the amount of C-PERM decreased substantially in untreated and cells treated with $1 \mu\text{M}$ PDBu (Figure 2D). Furthermore, the N-ERMAD or N-ERMAD(E244K) both caused an inhibition of C-PERM, indicating a dominant inhibition of endogenous ERM protein activation. Confocal microscopy analyses demonstrate a clear decrease in the amount of endogenous ezrin in the periphery of N-ERMAD(E244K)-expressing cells compared with untransfected cells within the same field of view. Further, the phalloidin staining showed a clear increase in the amount of F-actin in the ruffles after PKC stimulation, which was reduced in the presence of ERMAD(E244K) (see Supplementary Figure S1). Together, these data indicate a molecular mechanism for dominant inhibition by N-ERMAD through interacting with ERM-binding molecules, in addition to the effect of direct binding to the C-ERMAD in endogenous ERM proteins.

N-ERMAD(E244K) Specifically Affects the Activity of the Small GTPase Cdc42

Members of the family of small GTPases Cdc42 and Rac have been shown to have a critical function in the control of

the membrane protrusive activity and subsequently cell migration in a number of cell types (Raftopoulos and Hall, 2004). We therefore examined the functional behavior of Cdc42 and Rac in MDA-MB-231 cells in the presence of full-length ezrin or N-ERMAD(E244K). Cells expressing PAK1-GFP and Cdc42-myc in the absence or presence of either full-length ezrin or N-ERMAD(E244K) were left unstained or were labeled after fixation with an anti-myc-Cy3 IgG and then subjected to multiphoton FLIM to measure FRET efficiency between GFP and Cy3 (Parsons *et al.*, 2005). The detection of FRET between a GFP donor and a Cy3 by FLIM requires a spatial separation between the fluorophores of no more than 9 nm (Bastiaens and Jovin, 1996) and results in a shortening of the GFP (donor) fluorescence lifetime (τ). In the unstained cells that coexpress full-length ezrin, the control average lifetime of PAK1-GFP alone was 2.26 ns (top left panels of Figure 3A). In the presence of anti-myc-Cdc42 Cy3 acceptor, a significant reduction in GFP lifetime was observed, particularly in the peripheral cell protrusions (average $\tau = 1.91$ ns; FRET efficiency 15.8%; midleft panels, Figure 3A). In the presence of N-ERMAD(E244K), the FRET efficiency between PAK1-GFP and anti-myc-Cdc42 Cy3 acceptor was significantly reduced (Eff = 9.8%), demonstrating that the N-ERMAD(E244K) is altering the capacity of Cdc42 to interact with its downstream effector PAK1 (bottom left panels, Figure 3A). The N-ERMAD(E244K) did not have any effect upon the FRET between PAK1-GFP and Rac1-myc-Cy3 (right panels, Figure 3A), suggesting that the dominant inhibition of ERM function by N-ERMAD(E244K) specifically targets the activity of Cdc42. Biochemical PBD pull-down experiments demonstrated that the amount of GTP-bound Cdc42 in MDA-MB-231 cells was significantly reduced in the presence of N-ERMAD(E244K) compared with full-length ezrin (marked with an asterisk in Figure 3C). In agreement with results from the FRET/FLIM analysis, the amount of GTP-bound Rac was unaffected by the presence of N-ERMAD(E244K) (Figure 3C). The amount of GTP-bound RhoA in MDA-MB-231 breast carcinoma cells (which do not form noticeable stress fibers or focal adhesions) is below the detection limit of GST-Rhotekin pull-down assays, irrespective of the presence of N-ERMAD(E244K) (data not shown). From these data we conclude that the presence of N-ERMAD(E244K) specifically disrupts the interaction of Cdc42 with its downstream effector PAK1 and decreases the GTP-bound fraction of Cdc42 without altering the activity of Rac1.

N-ERMAD(E244K) Alters the Migratory Potential of MDA-MB-231 Cells

To test the potential role of N-ERMAD(E244K) in regulating Cdc42-driven cell motility, we compared random migratory potential of MDA-MB-231 cells transduced with N-ERMAD(E244K) or transfected with RNAi against Cdc42. Transfection of siRNA against Cdc42 lead to >90% reduction in Cdc42 expression (Figure 4A), with no alterations in basal expression levels of endogenous Rac1 or HSP70. The substantial reduction in Cdc42 expression was consistently observed up to 64 h after transfection (Figure 4A). In random migration assays, control MDA-MB-231 cells exposed to Chariot alone were highly motile and exhibited a polarized morphology, with formation of lamellipodia in the direction of migration (Figure 4B, top left panel). Quantitative analysis showed that the average speed of $26.5 \pm 0.9 \mu\text{m/h}$ for control cells significantly decreased to $19.9 \pm 0.7 \mu\text{m/h}$ ($p < 0.001$, $n = 95$) for N-ERMAD(E244K)-transduced MDA-MB-231 cells, indicating that the presence of N-ERMAD(E244K) in cells changes the migratory behavior, possibly through altering the ability to adopt a polarized cell morphology.

Figure 3 (cont). Cell lysates were incubated with $10 \mu\text{g}$ of GST-PBD and Western blotted with anti-Cdc42 (top panels) or anti-Rac (bottom panels). Data shown are representative of three independent experiments.

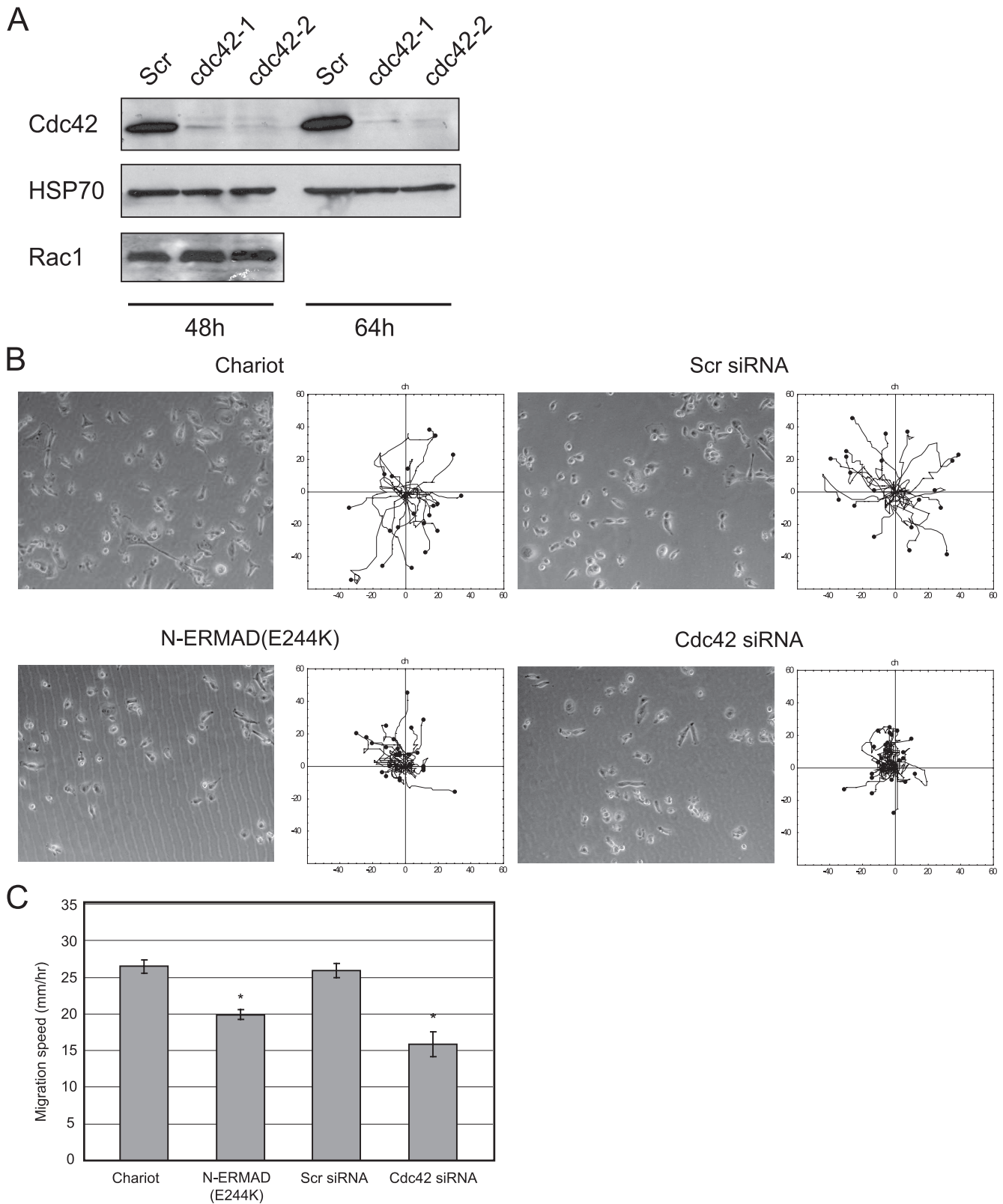
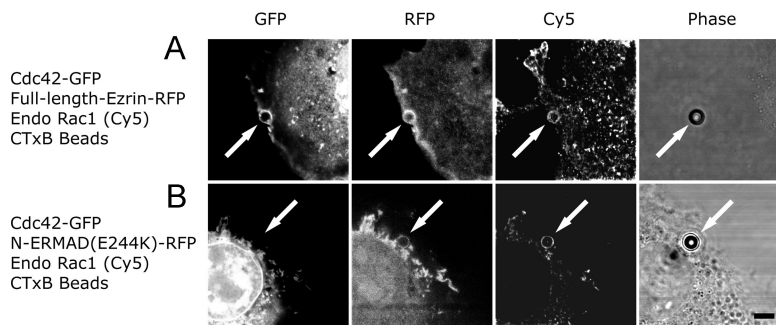


Figure 4. N-ERMAD(E244K) and Cdc42 regulates random migration of MDA-MB-231 cells. (A) Expression of Cdc42, HSP70, or Rac1, 48 or 64 h after transfection with scramble control RNAi (Scr) or either Cdc42-1 RNAi (Cdc42-1) or Cdc42-2 RNAi (Cdc42-2). Data shown are representative of three independent experiments. (B) Random cell migration of MDA-MB-231 cells transfected with Chariot alone (top left panel), purified N-ERMAD(E244K) protein (bottom left panel), or transfected with scramble RNAi (top right panel) or Cdc42 RNAi (bottom right panel) 48 h before recording. The track plots show all the cell trajectories during the entire time course of 2 h. Track plots are representative of three independent experiments. Representative phase-contrast images taken from a time-lapse movie at time = 0 are shown from each condition. (C) The migration speed of each cell is shown as mean \pm SEM; * $p < 0.001$, $n \geq 49$ cells, compared with control conditions. Data shown are representative of two independent experiments.



Rac1 (top panel) or anti-Dbl and anti-Rac1 (bottom panel). Cells were imaged by confocal microscopy. Bar, 10 μm .

Figure 5. (A) Cdc42 recruitment to lipid rafts is inhibited by N-ERMAD(E244K). Beads coated with 10 μM cholera toxin-B subunit were added to MDA-MB-231 cells expressing Wt-Cdc42-GFP, and full-length ezrin-mRFP1 or N-ERMAD(E244K)-mRFP1 and incubated for 30 min at 37°C. On fixation, cells were stained with antibodies to endogenous Rac1 followed by Cy5-conjugated secondary antibodies. Confocal imaging was performed to evaluate the specific recruitment to GM1 containing microdomains indicated by arrows. Bar, 5 μm . (B) CTxB coated beads were added to MDA-MB-231 cells alone or expressing N-ERMAD(E244K)-mRFP1 for 30 min. Cells were fixed and stained with anti-ezrin, anti-Dbl and anti-

MDA-MB-231 control cells transfected with scramble siRNA showed similar phenotype as untransfected cells with an average speed of $25.9 \pm 1.0 \mu\text{m}/\text{h}$ (Figure 4C). On knock-down of Cdc42 expression, the MDA-MB-231 cells showed a lack of polarized morphology and significantly reduced average cell speed of $15.9 \pm 1.7 \mu\text{m}/\text{h}$ (in comparison to chariot alone control cells; Figure 4C; $p < 0.001$, $n = 50$), similar to that seen in cells transduced with N-ERMAD(E244K).

N-ERMAD(E244K) Inhibits the Recruitment of Cdc42 But Not Rac1 to Lipid Rafts

GM1-containing lipid rafts are involved in integrin-mediated localization of Rac1 and subsequent cell adhesion signaling (del Pozo *et al.*, 2004). Recent data have also detected the presence of ERM proteins in lipid rafts using mass spectrometry (Foster *et al.*, 2003; Li *et al.*, 2003); therefore we were interested to test whether ezrin could play a role in the activation of Cdc42 within these domains and indeed if the presence of N-ERMAD(E244K) affects the recruitment of Cdc42 to the lipid rafts via dominant inhibition of ERM proteins. Localized clustering of GM1-containing lipid rafts promoted by the CTxB-coated beads led to the recruitment of Cdc42, full-length ezrin, as well as recruitment of endogenous Rac1 to the lipid raft microdomains (Figure 5, top panels). However, in the presence of N-ERMAD(E244K), the recruitment of Cdc42 to the lipid rafts was completely abolished, although N-ERMAD(E244K) itself was localized to the beads (Figure 5, bottom panels). Recruitment of Rac1 to the CTxB-coated beads was unaltered in the presence of N-ERMAD(E244K) (Figure 5, bottom panels). These data demonstrate that N-ERMAD(E244K) inhibits the targeting of Cdc42 to lipid rafts, providing a potential mechanism for regulation of its activity, without affecting the recruitment of Rac1.

N-ERMAD(E244K) Disrupts the Morphological Reorganization Induced by onco-Dbl

Activation of small GTPases is catalyzed by GEFs responsible for the GDP-GTP exchange (review see Rossman *et al.*, 2005). As we identified a functional role of ERM proteins in the local recruitment and activation of Cdc42, we were interested to test the role of ERM proteins in modulating GEF activity and behavior. We analyzed the morphological changes in MDA-MB-231 cells after overexpression of a panel of GEFs: the Cdc42-specific Rho GEF FGD1 and the Cdc42/Rho-specific GEF onco-Dbl (Olson *et al.*, 1996); the Rac-specific GEF Tiam1 (constitutively activated by an N-terminal deletion; Michiels *et al.*, 1997); and the Rho-specific GEF p190RhoGEF (van Horck *et al.*, 2001). Expression of FGD1 in MDA-MB-231 cells induces formation of filopodia and membrane ruffles (Figure 6A, top

panel left). Coexpression of N-ERMAD(E244K) with FGD1 resulted in formation of filopodia, suggesting that N-ERMAD(E244K) is unable to inhibit the activation of Cdc42 induced by overexpression of FGD1 (Figure 6A, top panel right). In the presence of onco-Dbl, an increase in membrane ruffling and lamellipodia spreading, similar to what was described previously (Olson *et al.*, 1996), is observed (Figure 6A, middle panel right). In contrast, cells coexpressing both onco-Dbl and N-ERMAD(E244K) rounded up and displayed no apparent ruffling (Figure 6B, middle panel left), indicating that N-ERMAD(E244K) is altering the ability of onco-Dbl to stimulate lamellipodial spreading, although not sufficient to completely block morphological transformation by onco-Dbl as observed in rounding of the cells. The expression of the constitutive active form of Tiam1 (C1199) induced the formation of membrane ruffles as previously described (Michiels *et al.*, 1997), and cells expressing both Tiam1 (C1199) and N-ERMAD(E244K) showed a similar increase in lamellipodia formation (Figure 6A, bottom panel). Morphological quantifications revealed a significant decrease in cell area (spreading) only upon coexpression of N-ERMAD(E244K) and onco-Dbl, where onco-Dbl-expressing cells have an average cell area of $984.2 \pm 75 \mu\text{m}^2$, and cells coexpressing onco-Dbl and N-ERMAD(E244K) showed an average cell area of $229.5 \pm 10 \mu\text{m}^2$ (Figure 6B; $p < 0.001$, $n = 11$ cells). Coexpression of N-ERMAD(E244K) alone, or in the presence of Tiam1(C1199) or FGD1, showed no significant alteration in cell area (Figure 6B). Expression of the Rho-specific GEF p190RhoGEF in cells stimulated F-actin reorganization and the formation of stress fibers (Figure 6C, top panel), and the reorganization of F-actin was independent of the presence of N-ERMAD(E244K) (Figure 6C, bottom panel). Together, these data indicate that N-ERMAD(E244K) specifically inhibits the morphological effect, i.e., lamellipodial spreading induced by an expression of onco-Dbl GEF activity, but not other GEFs such as FGD1, Tiam1, or p190RhoGEF.

To verify that these morphological changes were dependent on the activity of Cdc42, we coexpressed a constitutively active form of Cdc42 (V12Cdc42-GFP) together with onco-Dbl-myc and full-length ezrin-mRFP1 or N-ERMAD(E244K)-mRFP1. Expression of V12Cdc42 in the presence of onco-Dbl and full-length ezrin did not alter the cellular morphology compared with onco-Dbl and full-length ezrin alone (Figure 7A). However, expression of V12Cdc42 in the presence of onco-Dbl and N-ERMAD(E244K) stimulated a dramatic increase in membrane ruffling and lamellipodial formation (Figure 7A), in contrast to the round morphology induced by coexpression of onco-Dbl and N-ERMAD(E244K) alone, demonstrating that a constitutively active form of Cdc42 has the ability to rescue the inhibition of the onco-Dbl-induced phenotype by N-ERMAD(E244K). Quantification of pheno-

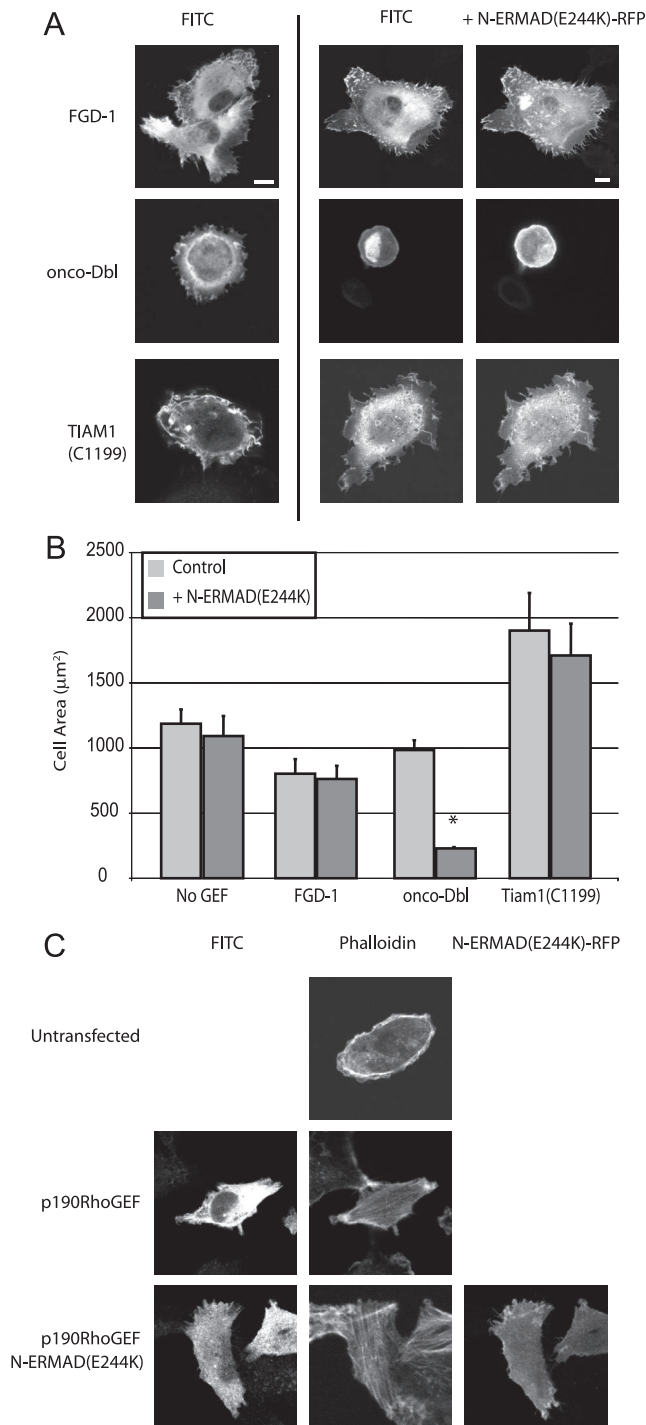


Figure 6. onco-Dbl induced morphological changes is dependent on functional ERM proteins. (A) MDA-MB-231 cells were microinjected with cDNAs encoding FGD1-myc, onco-Dbl-myc, or HA-Tiam1-(C1199) alone or together with N-ERMAD(E244K)-mRFP1 as indicated, and incubated at 37°C for 6 h, fixed, and stained with FITC-conjugated antibodies against myc (FGD1 and Dbl) or HA (Tiam1(C1199)). Bar, 5 µm. (B) Quantification of area of MDA-MB-231 cells as shown in (A). n = 10–15 cells. (C) Wild-type MDA-MB-231 cells or cells microinjected with cDNAs encoding HA-p190RhoGEF alone or together with N-ERMAD(E244K)-mRFP1 and incubated at 37°C for 6 h, fixed, and stained with Alexa633-conjugated Phalloidin and FITC-conjugated antibodies against HA.

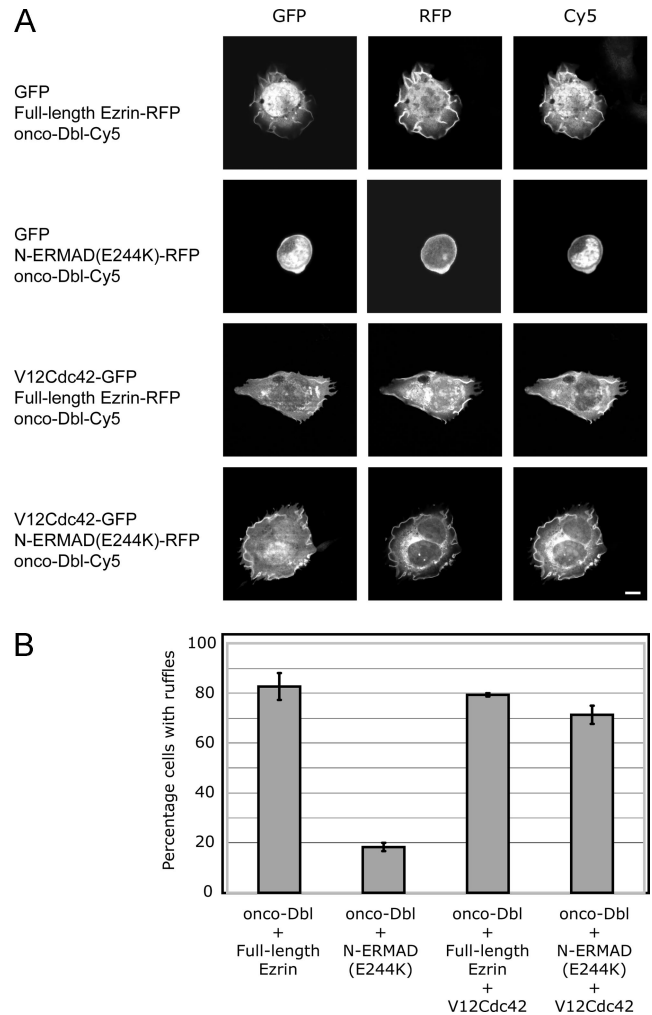


Figure 7. onco-Dbl induced morphological changes is dependent on activation of Cdc42. (A) MDA-MB-231 cells were microinjected with cDNAs encoding onco-Dbl-myc, GFP, or V12Cdc42-GFP and full-length ezrin-mRFP1 or N-ERMAD(E244K)-mRFP1 as indicated, incubated at 37°C for 6 h, fixed, and stained with Cy5-conjugated antibodies against myc. Bar, 5 µm. (B) Quantification of onco-Dbl induced morphological changes as observed in A. Cells were scored positive for containing membrane ruffles. Values are obtained from >60 cells per condition from three independent experiments and presented as mean ± SEM.

types confirmed the V12Cdc42 rescue of membrane ruffling activity (Figure 7B). Moreover, coexpression of onco-Dbl and a dominant inhibitory form of Cdc42 (N17Cdc42) results in a rounded cell morphology similar to cells coexpressing onco-Dbl and N-ERMAD(E244K) (data not shown). To verify the Cdc42 dependency in Dbl-induced membrane ruffling, we examined the cell morphology in Cdc42 knockdown MDA-MB-231 cells. Expression of onco-Dbl in Cdc42 knockdown cells resulted in a rounded morphology, whereas the onco-Dbl expression in cells transfected with control siRNA induced formation of membrane ruffles (Figure 8), similar to cells expressing onco-Dbl alone (Figure 6A). These experiments demonstrate that the cytoskeletal rearrangement controlled by Dbl can be prevented by expression of N-ERMAD(E244K) and suggest a functional role of ERM proteins in the regulation of Dbl GEF activity. Furthermore, data obtained using Cdc42-specific siRNA demonstrate a specific role of Cdc42 in the process of Dbl-dependent morphological rearrangement and thereby add functional

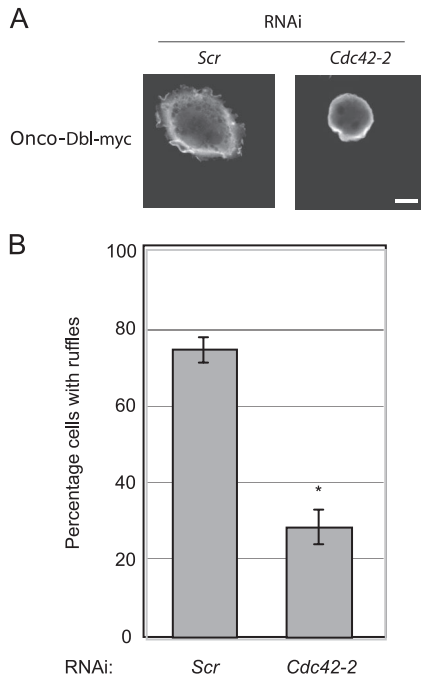


Figure 8. onco-Dbl induced morphological changes is dependent expression of Cdc42. (A) MDA-MB-231 cells were transfected with scramble RNAi (Scr) or Cdc42 RNAi (Cdc42-2) 48 h before micro-injected with cDNAs encoding onco-Dbl-myc and incubated at 37°C for 6 h, fixed, and stained with Cy3-conjugated antibodies against myc. Bar, 5 μ m. (B) Quantification of onco-Dbl induced morphological changes as observed in A. Cells were scored positive for containing membrane ruffles. Values are obtained from >60 cells per condition from three independent experiments and presented as mean \pm SEM.

evidence that corroborate our hypothesis that ERM proteins are critically involved in the Dbl-dependent regulation of Cdc42 activity.

Expression of N-ERMAD(E244K) Inhibits the Recruitment of Dbl to the Plasma Membrane

Activation of small GTPases by Rho GEFs is orchestrated by a combination of GDP/GTP exchange catalyzed by the Dbl-homology (DH) domain and spatial membrane localization directed by the Pleckstrin-homology (PH) domain (reviewed by Rossman *et al.*, 2005). As ezrin has previously been shown to interact with Dbl via the PH domain (Vanni *et al.*, 2004), we analyzed the affects of N-ERMAD(E244K) on the subcellular localization of Dbl as a potential target for inhibiting Cdc42 activation. Endogenous Dbl is predominantly localized to the plasma membrane and in the cytoplasm overlapping with the localization of full-length ezrin (Figure 9A), similar to that reported previously (Vanni *et al.*, 2004). In the presence of N-ERMAD(E244K), the endogenous Dbl failed to be recruited to the plasma membrane and showed no colocalization with N-ERMAD(E244K) (Figure 9A). Analysis of recruitment to lipid raft microdomains in cells after incubation with CTxB-coated beads demonstrated a recruitment of endogenous Dbl, ezrin, and Rac1 to GM1-containing microdomains (Figure 9B). In contrast, when N-ERMAD(E244K) was expressed there was no recruitment of Dbl to the GM1-containing microdomains, whereas the localization of N-ERMAD(E244K) and Rac1 were detectable (Figure 9B). This demonstrates that the presence of N-ERMAD(E244K) inhibits the translocation of Dbl to the

plasma membrane and to lipid raft microdomains, suggesting a requirement of functional ERM proteins for proper spatial localization of Dbl.

Activated Ezrin Restores the Plasma Membrane Targeting of Dbl in the Presence of N-ERMAD(E244K)

To identify the conformational requirement for ERM binding to endogenous Dbl, we performed immunoprecipitation experiments with the WT, the phosphomimetic (T567D), or the nonphosphorylatable (T567A) mutant form of ezrin and assessed the amount of Dbl that can be coprecipitated. These experiments showed an increased association of endogenous Dbl with ezrin(T567D) compared with WT ezrin, whereas no binding of Dbl to ezrin(T567A) was detected (Figure 10A). This demonstrates that ezrin associates with Dbl only in its open conformation. Furthermore, immunoprecipitation of endogenous ezrin from MDA-MB-231 cells revealed that a cocomplex including Dbl is formed in vivo (Figure 10B). Stimulation of cells by PDBu, which increases the amount of C-terminally phosphorylated ERM (as shown in Figure 2B) was shown to increase the binding of Dbl to ezrin in MDA-MB-231 cells (Figure 10B). Transduction of purified N-ERMAD(E244K) into MDA-MB-231 cells, however, decreased the interaction between Dbl and ezrin that is induced by PKC activation (Figure 10B). We postulated that the N-ERMAD(E244K)-mediated inhibition of endogenous Dbl recruitment to the plasma membrane (Figure 9A) was caused by a dominant inhibition of C-terminal phosphorylation of endogenous ERM proteins and that this effect should be reversed by overexpression of the phosphomimetic (T567D) form of ezrin. This is demonstrated in Figure 10C where the coexpression of ezrin(T567D), rather than the nonphosphorylatable (T567A) form, when cotransfected with N-ERMAD(E244K) in a 2:1 ratio, was able to restore the localization of endogenous Dbl to the plasma membrane.

DISCUSSION

In previous studies, we have shown ezrin to be an important mediator of breast cancer cell migration (Ng *et al.*, 2001) and a number of recent articles have highlighted the significant contribution of ezrin to the clinical development of metastasis in both osteosarcoma and rhabdomyosarcoma (Khanna *et al.*, 2004; Yu *et al.*, 2004; Elliott *et al.*, 2005). Mechanistically, ERM proteins have been implicated in the regulation of the Rho family of small GTPases either through inhibition of the Rho-specific GDP dissociation inhibitor RhoGDI (Takahashi *et al.*, 1997) or through interaction with the Cdc42/Rho-specific guanine exchange factor Dbl (Vanni *et al.*, 2004). The functional consequence of the ERM-Dbl complex on Rho GTPase activity has to date however only been demonstrated for RhoA. For instance, in the context of uropod formation in lymphocytes, the C-terminal threonine-phosphorylated form of full-length ezrin was shown to associate with Dbl through its NH₂-terminal domain and causes Rho activation (Lee *et al.*, 2004). Here we define a novel mechanism by which ezrin is important and necessary for spatial activation of Cdc42 in MDA-MB-231 cells. We observe that Dbl is recruited to GM1-positive microdomains in the plasma membrane in an ERM-dependent manner, and that onco-Dbl induced morphological changes are dependent on Cdc42 and functional ERM proteins. This suggests a mechanism whereby Dbl interacts with ezrin and/or other ERM proteins and is thereby recruited to the plasma membrane and to lipid raft microdomains, enabling a localized activation of Cdc42. Furthermore, these breast cancer cells do not have a detectable amount of GTP-bound RhoA and do not

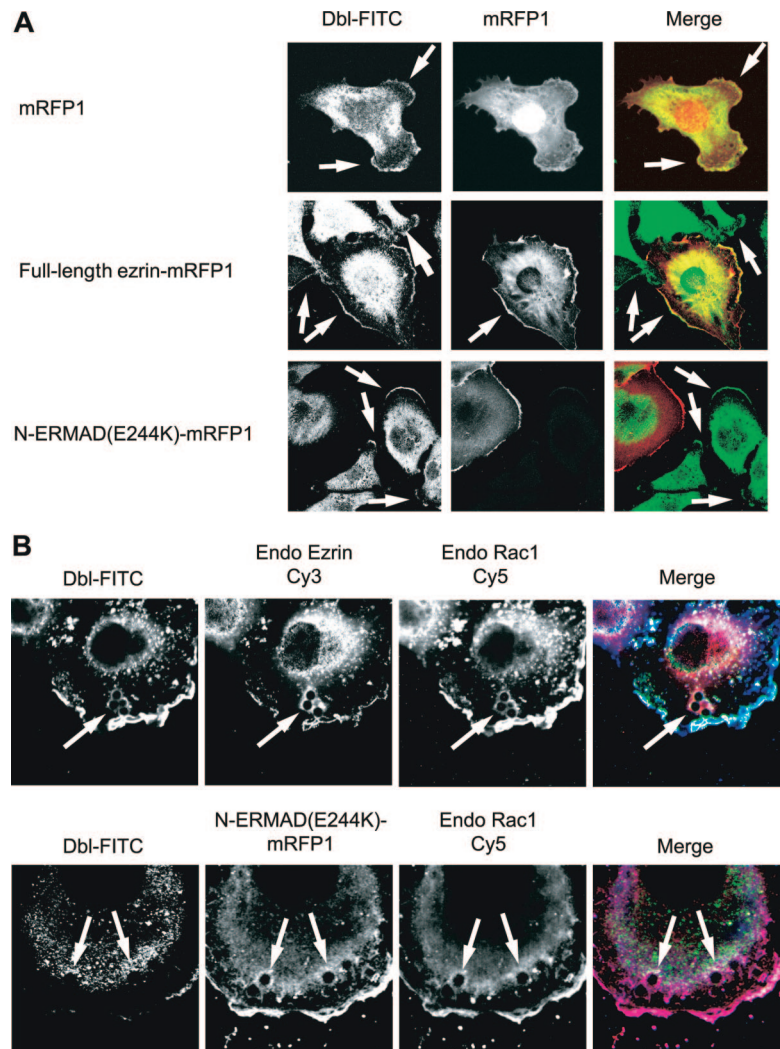


Figure 9. Expression of N-ERMAD(E244K) inhibits recruitment of Dbl to the plasma membrane and the lipid raft. (A) MDA-MB-231 cells expressing full-length ezrin-mRFP1 or N-ERMAD(E244K)-mRFP1 were fixed and stained with anti-Dbl followed by FITC-conjugated secondary antibodies. Cells were imaged by confocal microscopy. (B) CTxB-coated beads were added to MDA-MB-231 cells alone or expressing N-ERMAD(E244K)-mRFP1 for 30 min. Cells were fixed and stained with anti-ezrin, anti-Dbl, and anti-Rac1 (top panel) or anti-Dbl and anti-Rac1 (bottom panel). Cells were imaged by confocal microscopy. Bar, 10 μ m.

ordinarily form stress fibers or focal adhesions. The effect of N-ERMAD(E244K), through an abrogation of endogenous ERM-Dbl association, is therefore likely to be specific via a down-regulation of Cdc42 activity.

Previous experiments detected ERM proteins in lipid rafts using quantitative proteomic mass spectrometry analyses (Foster *et al.*, 2003; Li *et al.*, 2003). Using density gradient fractionation techniques and caveolin as a lipid raft marker, we found only a small fraction of endogenous ezrin to localize to the fractions that contain caveolin (#6-#8; Supplementary Figure S2). The low percentage of total ezrin residing in lipid rafts at any one time makes relatively insensitive biochemical techniques such as sucrose gradient fractionation unsuitable for a quantitative analysis of changes in distribution.

On the basis of structure-function analyses and BIAcore assays, we have modified the dominant inhibitory strategy, which is based on ezrin N-ERMAD, and created a point mutant (E244K) that has an impaired ability to bind to the C-ERMAD. This mutated N-ERMAD domain retains the ability to inhibit PKC-mediated cell migration in a dominant negative manner. Notably, the C-terminal threonine phosphorylation of endogenous ERM induced by phorbol ester was inhibited by both N-ERMAD and N-ERMAD(E244K) despite the 400-fold reduction of N-

ERMAD:C-ERMAD affinity caused by the point mutation. Hence, for the first time, we have demonstrated that the functional inhibition by the N-ERMAD domain is enhanced despite a decreased association with endogenous ERM proteins. As both N-ERMAD and N-ERMAD(E244K) locate at the plasma membrane, we postulate that the decrease in N-ERMAD:C-ERMAD association increases the availability of N-ERMAD(E244K) and that the dominant inhibition is instead achieved by abrogating the interaction between endogenous ERM and various N-ERMAD-interacting partners that are involved in the conformational activation of ERM proteins (Fievet *et al.*, 2004; reviewed in Bretscher *et al.*, 2002). The T567D form rescues because it does not require the activation machinery, i.e., it is already in the open conformation to bind to Dbl at the right location, where the membrane is locally tethered to the cytoskeleton. Potential N-ERMAD-interacting partners that contribute to the activation process include the various protein kinases that phosphorylate the conserved C-terminal threonine (myotonic dystrophy kinase-related Cdc42-binding kinase [Nakamura *et al.*, 2000], protein kinase C α [Ng *et al.*, 2001], and Nck-interacting kinase [Baumgartner *et al.*, 2006]) as well as the phosphoinositide PIP₂ (Fievet *et al.*, 2004). PIP₂ (IP₃ head) binding was shown to require several lysine residues from subdomains

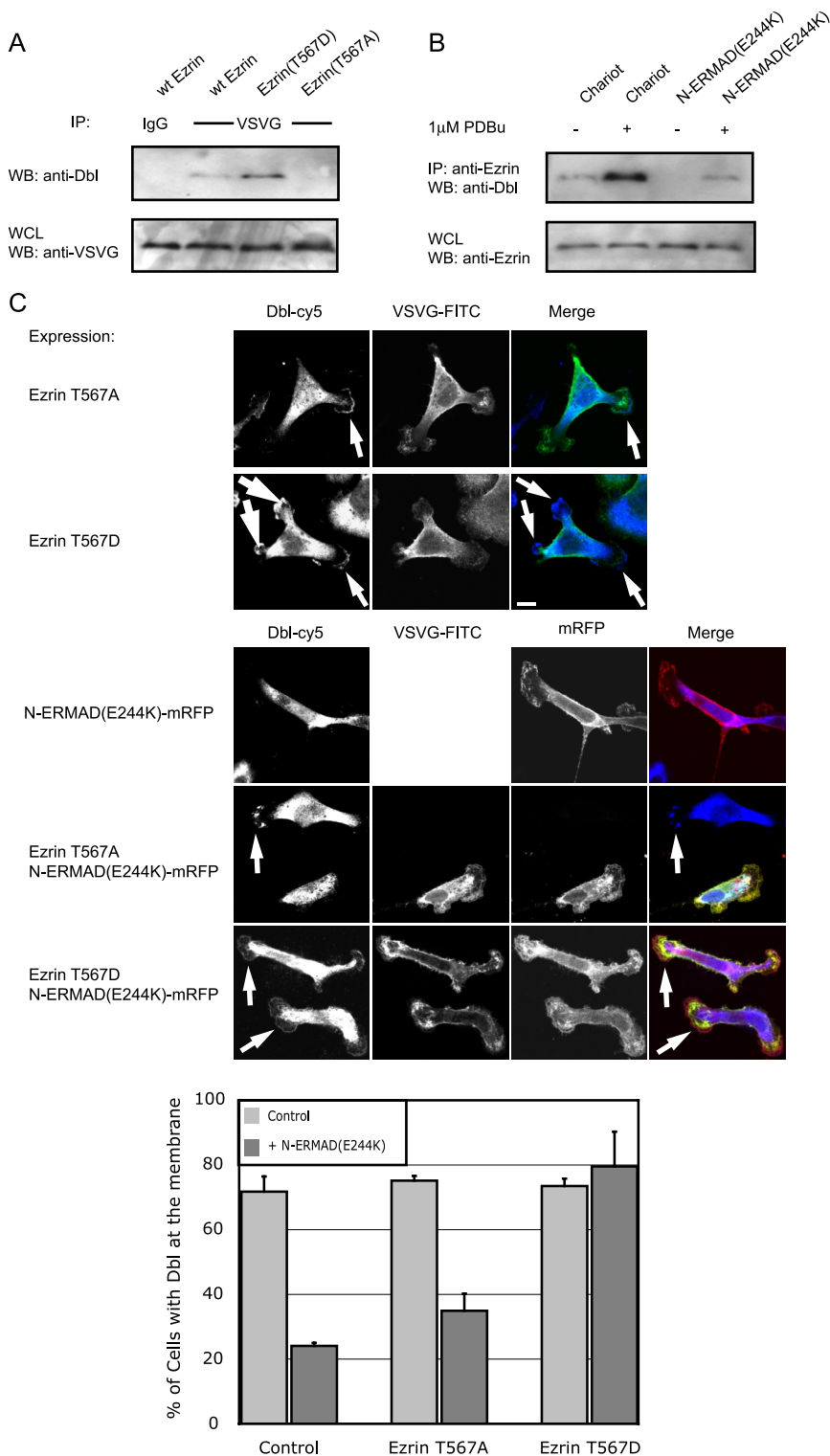


Figure 10. Activated ezrin interacts and recruits endogenous Dbl to the membrane. (A) Coimmunoprecipitation of VSVG-ezrin and Dbl from MDA-MB-231 cells transfected with WT ezrin (lane 1 and 2), ezrin(T567D) (lane 3), or ezrin(T567A) (lane 4), using control IgG, (lane 1) or mAb anti-VSVG. Endogenous Dbl was detected from coimmunoprecipitations using anti-Dbl rabbit serum (top panel), and expression levels were assessed from whole cell lysates (WCL) using mAb anti-VSVG (bottom panel). (B) Coimmunoprecipitation of ezrin and Dbl from untreated MDA-MB-231 cells or MDA-MB-231 cells treated with 1 μ M PDBu for 20 min at 37°C, or transfected with purified N-ERMAD(E244K) protein using Chariot for 2 h at 37°C. Endogenous ezrin was immunoprecipitated from cell lysates, and coimmunoprecipitation of endogenous Dbl was detected using anti-Dbl rabbit serum. (C) Confocal immunofluorescence images of endogenous Dbl distribution in MDA-MB-231 cells expressing ezrin(T567A)-VSVG or ezrin(T567D)-VSVG alone (top panels), and in the presence of N-ERMAD(E244K)-mRFP1 (bottom panels; various VSVG-ezrin plasmids co-transfected with N-ERMAD(E244K) in a 2:1 ratio) using an anti-Dbl rabbit serum and Cy5-conjugated secondary, plus an anti-VSVG mAb and FITC-conjugated anti-mouse secondary. Arrows indicate Dbl localization at the membrane. Bar, 10 μ m.

A and C of N-ERMAD, which form the positively charged molecular surface to interact with the negatively charged membrane inositol polyphosphates and, in the absence of PIP₂, moesin does not bind CD44 *in vitro* (Hamada *et al.*, 2000). Although the effect of the E244K on PIP₂ binding was not formally tested, the non-PIP₂-binding mutated (K253/254N, K262/263N) form of ezrin N-ERMAD was shown to be restricted to the cytoplasm, an effect that we

did not observe with the E244K mutation. The identification of the precise binding protein that is "titrated" away by the N-ERMAD(E244K) will be the subject of further investigation.

Expression of N-ERMAD(E244K) resulted in a decrease of Cdc42 recruitment to lipid rafts. This was in addition to a decrease in the localized association of Cdc42 with its downstream effector PAK, and a global reduction in ac-

tive, GTP-bound Cdc42. No changes were observed in the closely related GTPase Rac1, which led us to further investigate specific GEFs involved in regulation of GTPase activity. We identified Dbl as an upstream activator and exchange factor specific to Cdc42 in MDA-MB-231 cells, which was partially inhibited by the presence of N-ERMAD(E244K). Coexpression of N-ERMAD(E244K) could not reverse the phenotype after expression of onco-Dbl or mimic the phenotype of N-ERMAD(E244K) expression alone, possibly due to the much enhanced activity state and the decrease in protein turnover of onco-Dbl when compared with the endogenous proto-Dbl (Ron *et al.*, 1989; Kamynina *et al.*, 2007). Conversely, no changes were detected when analyzing the cell morphology induced by Cdc42-specific FGD1, Rac-specific Tiam1, or Rho-specific p190RhoGEF, in the absence or presence of N-ERMAD(E244K). Here we report that the morphological changes induced by onco-Dbl are dependent on the downstream effector Cdc42, and notably, the function of ERM proteins.

N-ERMAD(E244K) expression inhibits both the correct spatial recruitment of Dbl to the plasma membrane as well as the lipid raft recruitment and activation of Cdc42. Furthermore, in support of our hypothesis that the N-ERMAD(E244K)-mediated inhibition of endogenous Dbl recruitment to the plasma membrane was caused by a dominant inhibition of C-terminal phosphorylation of endogenous ERM proteins, this effect was shown to be reversed by overexpression of the phosphomimetic (T567D), rather than the nonphosphorylatable (T567A) form of ezrin. Together, these findings suggest that the active (i.e., C-terminally phosphorylated) form of ERM proteins, through forming a protein complex with Dbl, contributes toward Cdc42 activation in the correct subcellular localization, in response to promigratory signals. The activation of lipid raft localized Cdc42 (and its downstream effector PAK1; Krautkramer *et al.*, 2004) in turn can stimulate rapid lipid raft patch accumulation (Golub and Caroni, 2005) and hence promote actin cytoskeleton accumulation and sustained protrusive activity at the leading edge.

Correct subcellular localization of activated species of GTPases is emerging as a common mechanism in the regulation of different dynamic cellular processes. Rap1 promotes cell spreading by localizing the Rac-specific GEFs VAV2 and Tiam1 to the plasma membrane and concurrent Rac1 activation (Arthur *et al.*, 2004). Moreover, inactivation of Rap1 can inhibit cell spreading promoted by constitutive active forms of VAV2 and Tiam1. This indicates that even the VAV2/Tiam1-promoted increase in Rac1 activity is not sufficient to promote cell spreading highlighting the significance of proper subcellular localization (Arthur *et al.*, 2004). In *Saccharomyces cerevisiae*, targeting of the Cdc42p-specific GEF Cdc24p to the incipient bud site is essential for the recruitment and activation of Cdc42p, and deletion of the Dbl-homology domain responsible for targeting Cdc24p to the budding site is lethal and unable to complement the growth defects of *Cdc24Δ* cells (Ziman and Johnson, 1994; Toenjes *et al.*, 1999; Shimada *et al.*, 2004). This indicates an evolutionarily conserved mechanism for proper localized GTPase activation. In the work presented here, we suggest a similar mechanism whereby ERM proteins are involved in the activation of Cdc42 in lipid raft microdomains at the leading edge of migrating cancer cells, via recruitment of the Cdc42/Rho-specific GEF Dbl.

ACKNOWLEDGMENTS

We thank support from the Cancer Research UK in the form of a project grant (SP2607/0101). M.P. is a Royal Society University Research Fellow. A.B. is funded by the National Asthma Campaign. T.N. is supported by an endowment fund from the Richard Dimbleby Cancer Fund to King's College London. The multiphoton FLIM system was built with support from both the Medical Research Council CoOperative Group Grant G0100152 ID 56891 and an UK Research Councils Basic Technology Research Programme Grant GR/R87901/01.

REFERENCES

- Algrain, M., Turunen, O., Vaheri, A., Louvard, D., and Arpin, M. (1993). Ezrin contains cytoskeleton and membrane binding domains accounting for its proposed role as a membrane-cytoskeletal linker. *J. Cell Biol.* *120*, 129–139.
- Amieva, M. R., Litman, P., Huang, L., Ichimaru, E., and Furthmay, H. (1999). Disruption of dynamic cell surface architecture of NIH3T3 fibroblasts by the N-terminal domains of moesin and ezrin: in vivo imaging with GFP fusion proteins. *J. Cell Sci.* *112*, 111–125.
- Andreoli, C., Martin, M., Le Borgne, R., Reggio, H., and Mangeat, P. (1994). Ezrin has properties to self-associate at the plasma membrane. *J. Cell Sci.* *107*, 2509–2521.
- Arthur, W. T., Quilliam, L. A., and Cooper, J. A. (2004). Rap1 promotes cell spreading by localizing Rac guanine nucleotide exchange factors. *J. Cell Biol.* *167*, 111–122.
- Barret, C., Roy, C., Montcourrier, P., Mangeat, P., and Niggli, V. (2000). Mutagenesis of the phosphatidylinositol 4,5-bisphosphate (PIP(2)) binding site in the NH(2)-terminal domain of ezrin correlates with its altered cellular distribution. *J. Cell Biol.* *151*, 1067–1080.
- Bastiaens, P. I., and Jovin, T. M. (1996). Microspectroscopic imaging tracks the intracellular processing of a signal transduction protein: fluorescently-labeled protein kinase C beta I. *Proc. Natl. Acad. Sci. USA* *93*, 8407–8412.
- Baumgartner, M., Sillman, A. L., Blackwood, E. M., Srivastava, J., Madson, N., Schilling, J. W., Wright, J. H., and Barber, D. L. (2006). The Nck-interacting kinase phosphorylates ERM proteins for formation of lamellipodium by growth factors. *Proc. Natl. Acad. Sci. USA* *103*, 13391–13396.
- Bretscher, A., Edwards, K., and Fehon, R. G. (2002). ERM proteins and merlin: integrators at the cell cortex. *Nat. Rev. Mol. Cell Biol.* *3*, 586–599.
- Chambers, D. N., and Bretscher, A. (2005). Ezrin mutants affecting dimerization and activation. *Biochemistry* *44*, 3926–3932.
- Crepaldi, T., Gautreau, A., Comoglio, P. M., Louvard, D., and Arpin, M. (1997). Ezrin is an effector of hepatocyte growth factor-mediated migration and morphogenesis in epithelial cells. *J. Cell Biol.* *138*, 423–434.
- del Pozo, M. A., Alderson, N. B., Kioussis, W. B., Chiang, H. H., Anderson, R.G.W., and Schwartz, M. A. (2004). Integrins regulate Rac targeting by internalization of membrane domains. *Science* *303*, 839–842.
- Elliott, B. E., Meens, J. A., SenGupta, S. K., Louvard, D., and Arpin, M. (2005). The membrane cytoskeletal crosslinker ezrin is required for metastasis of breast carcinoma cells. *Breast Cancer Res.* *7*, R365–R373.
- Etienne-Manneville, S., and Hall, A. (2002). Rho GTPases in cell biology. *Nature* *420*, 629–635.
- Fievet, B. T., Gautreau, A., Roy, C., Del Maestro, L., Mangeat, P., Louvard, D., and Arpin, M. (2004). Phosphoinositide binding and phosphorylation act sequentially in the activation mechanism of ezrin. *J. Cell Biol.* *164*, 653–659.
- Foster, L. J., De Hoog, C. L., and Mann, M. (2003). Unbiased quantitative proteomics of lipid rafts reveals high specificity for signaling factors. *Proc. Natl. Acad. Sci. USA* *100*, 5813–5818.
- Golub, T., and Caroni, P. (2005). PI(4,5)P2-dependent microdomain assemblies capture microtubules to promote and control leading edge motility. *J. Cell Biol.* *169*, 151–165.
- Hamada, K., Shimizu, T., Matsui, T., Tsukita, S., and Hakoshima, T. (2000). Structural basis of the membrane-targeting and unmasking mechanisms of the radixin FERM domain. *EMBO J.* *19*, 4449–4462.
- Itoh, R. E., Kurokawa, K., Ohba, Y., Yoshizaki, H., Mochizuki, N., and Matsuda, M. (2002). Activation of rac and cdc42 video imaged by fluorescent resonance energy transfer-based single-molecule probes in the membrane of living cells. *Mol. Cell Biol.* *22*, 6582–6591.
- Kamynina, E., Kauppinen, K., Duan, F., Muakkassa, N., and Manor, D. (2007). Regulation of proto-oncogenic Dbl by chaperone-controlled, ubiquitin-mediated degradation. *Mol. Cell Biol.* *27*, 1809–1822.
- Khanna, C., Wan, X., Bose, S., Cassaday, R., Olomu, O., Mendoza, A., Yeung, C., Gorlick, R., Hewitt, S. M., and Helman, L. J. (2004). The membrane-

- cytoskeleton linker ezrin is necessary for osteosarcoma metastasis. *Nat. Med.* *10*, 182–186.
- Kozma, R., Ahmed, S., Best, A., and Lim, L. (1995). The Ras-related protein Cdc42Hs and bradykinin promote formation of peripheral actin microspikes and filopodia in Swiss 3T3 fibroblasts. *Mol. Cell. Biol.* *15*, 1942–1952.
- Krautkramer, E., Giese, S. I., Gasteier, J. E., Muranyi, W., and Fackler, O. T. (2004). Human immunodeficiency virus Type 1 Nef activates p21-activated kinase via recruitment into lipid rafts. *J. Virol.* *78*, 4085–4097.
- Lamb, R. F., Ozanne, B. W., Roy, C., McGarry, L., Stipp, C., Mangeat, P., and Jay, D. G. (1997). Essential functions of ezrin in maintenance of cell shape lamellipodial extension in normal and transformed fibroblasts. *Curr. Biol.* *7*, 682–688.
- Lee, J. H., Katakai, T., Hara, T., Gonda, H., Sugai, M., and Shimizu, A. (2004). Roles of p-ERM and Rho-ROCK signaling in lymphocyte polarity and uropod formation. *J. Cell Biol.* *167*, 327–337.
- Legg, J. W., Lewis, C. A., Parsons, M., Ng, T., and Isacke, C. M. (2002). A novel PKC-regulating mechanism controls CD44 ezrin association and directional cell motility. *Nat. Cell Biol.* *27*, 399–407.
- Leung, T., Chen, X. Q., Tan, I., Manser, E., and Lim, L. (1998). Myotonic dystrophy kinase-related Cdc42-binding kinase acts as a Cdc42 effector in promoting cytoskeletal reorganization. *Mol. Cell. Biol.* *18*, 130–140.
- Li, N., Mak, A., Richards, D. P., Naber, C., Keller, B. O., Li, L., and Shaw, A.R.E. (2003). Monocyte lipid rafts contain proteins implicated in vesicular trafficking and phagosome formation. *Proteomics* *3*, 536–548.
- Martin, M., Andreoli, C., Sahuquet, A., Montcourrier, P., Algrain, M., and Mangeat, P. (1995). Ezrin NH2-terminal domain inhibits the cell extension activity of the COOH-terminal domain. *J. Cell Biol.* *128*, 1081–1093.
- Michiels, F., Stam, J. C., Hordijk, P. L., Kammen, R. A., Stalle, L.R.-V., Feltkamp, C. A., and Collard, J. G. (1997). Regulated membrane localization of Tiam1, mediated by the NH2-terminal pleckstrin homology domain, is required for Rac-dependent membrane ruffling and C-Jun NH2-terminal kinase activation. *J. Cell Biol.* *137*, 387–398.
- Nakamura, N., Oshiro, N., Fukata, Y., Amano, M., Fukata, M., Kuroda, S., Matsuura, Y., Leung, T., Lim, L., and Kaibuchi, K. (2000). Phosphorylation of ERM proteins at filopodia induced by Cdc42. *Genes Cells* *5*, 571–581.
- Ng, T. *et al.* (2001). Ezrin is a downstream effector of trafficking PKC-integrin complexes involved in the control of cell motility. *EMBO J.* *20*, 2723–2741.
- Ng, T., Shima, D., Squire, A., Bastiaens, P. I., Gschmeissner, S., Humphries, M. J., and Parker, P. J. (1999). PKC α regulates beta1 integrin-dependent cell motility through association and control of integrin traffic. *EMBO J.* *18*, 3909–3923.
- Nobes, C. D., and Hall, A. (1995). Rho, rac, and cdc42 GTPases regulate the assembly of multimolecular focal complexes associated with actin stress fibers, lamellipodia, and filopodia. *Cell* *81*, 53–62.
- Nobes, C. D., and Hall, A. (1999). Rho GTPases control polarity, protrusion, and adhesion during cell movement. *J. Cell Biol.* *144*, 1235–1244.
- Olson, M. F., Pasteris, N. G., Gorski, J. L., and Hall, A. (1996). Faciogenital dysplasia protein (FGD1) and Vav, two related proteins required for normal embryonic development, are upstream regulators of Rho GTPases. *Curr. Biol.* *6*, 1628–1633.
- Parsons, M. *et al.* (2005). Spatially distinct binding of Cdc42 to PAK1 and N-WASP in breast carcinoma cells. *Mol. Cell. Biol.* *25*, 1680–1695.
- Parsons, M., and Ng, T. (2002). Intracellular coupling of adhesion receptors: molecular proximity measurements. In: *Methods in Cell Biology*, vol. 69, ed. J. Adams, San Diego: Academic Press, Chapter 212, 261–278.
- Pearson, M. A., Reczek, D., Bretscher, A., and Karplus, P. A. (2000). Structure of the ERM protein moesin reveals the FERM domain fold masked by an extended actin binding tail domain. *Cell* *101*, 259–270.
- Peter, M., Ameer-Beg, S. M., Hughes, M. K., Keppler, M. D., Prag, S., Marsh, M., Vojnovic, B., and Ng, T. (2005). Multiphoton-FLIM quantification of the EGFP-mRFP1 FRET pair for localization of membrane receptor-kinase interactions. *Biophys. J.* *88*, 1224–1237.
- Pietromonaco, S. F., Simons, P. C., Altman, A., and Elias, L. (1998). Protein kinase C- θ phosphorylation of moesin in the actin-binding sequence. *J. Biol. Chem.* *273*, 7594–7603.
- Raftopoulou, M., and Hall, A. (2004). Cell migration: Rho GTPases lead the way. *Dev. Biol.* *265*, 23–32.
- Reczek, D., Berryman, M., and Bretscher, A. (1997). Identification of EBP 50, a PDZ-containing phosphoprotein that associates with members of the ezrin-radixin-moesin family. *J. Cell Biol.* *139*, 169–179.
- Ridley, A. J., Schwartz, M. A., Burridge, K., Firtel, R. A., Ginsberg, M. H., Borisy, G., Parsons, J. T., and Horwitz, A. R. (2003). Cell migration: integrating signals from front to back. *Science* *302*, 1704–1709.
- Ron, D., Graziani, G., Aaronson, S. A., and Eva, A. (1989). The N-terminal region of proto-dbl down regulates its transforming activity. *Oncogene* *4*, 1067–1072.
- Rossmann, K. L., Der, C. J., and Sondek, J. (2005). GEF means go: turning on RHO GTPases with guanine nucleotide-exchange factors. *Nat. Rev. Mol. Cell Biol.* *6*, 167–180.
- Sahai, E., and Marshall, C. J. (2003). Differing modes of tumour cell invasion have distinct requirements for Rho/ROCK signalling and extracellular proteolysis. *Nat. Cell Biol.* *5*, 711–719.
- Shimada, Y., Wiget, P., Gulli, M. P., Bi, E., and Peter, M. (2004). The nucleotide exchange factor Cdc24p may be regulated by auto-inhibition. *EMBO J.* *23*, 1051–1062.
- Takahashi, K., Sasaki, T., Mammoto, A., Takaishi, K., Kameyama, T., Tsukita, S., and Takai, Y. (1997). Direct interaction of the Rho GDP dissociation inhibitor with ezrin/radixin/moesin initiates the activation of the Rho small G protein. *J. Biol. Chem.* *272*, 23371–23375.
- Toenjes, K. A., Sawyer, M. M., and Johnson, D. I. (1999). The guanine-nucleotide-exchange factor Cdc24p is targeted to the nucleus and polarized growth sites. *Curr. Biol.* *9*, 1183–1186.
- van Horck, F.P.G., Ahmadian, M. R., Haeusler, L. C., Moolenaar, W. H., and Kranenburg, O. (2001). Characterization of p190RhoGEF, a RhoA-specific guanine nucleotide exchange factor that interacts with microtubules. *J. Biol. Chem.* *276*, 4948–4956.
- Vanni, C., Parodi, A., Mancini, P., Visco, V., Ottaviano, C., Torrisi, M. R., and Eva, A. (2004). Phosphorylation-independent membrane relocation of ezrin following association with Dbl in vivo. *Oncogene* *23*, 4098–4106.
- Yonemura, S., Hirao, M., Doi, Y., Takahashi, N., Kondo, T., Tsukita, S., and Tsukita, S. (1998). Ezrin/radixin/moesin (ERM) proteins bind to a positively charged amino acid cluster in the juxta-membrane cytoplasmic domain of CD44, CD43, and ICAM-2. *J. Cell Biol.* *140*, 885–895.
- Yu, Y., Khan, J., Khanna, C., Helman, L., Meltzer, P. S., and Merlino, G. (2004). Expression profiling identifies the cytoskeletal organizer ezrin and the developmental homeoprotein Six-1 as key metastatic regulators. *Nat. Med.* *10*, 175–181.
- Ziman, M., and Johnson, D. I. (1994). Genetic evidence for a functional interaction between *Saccharomyces cerevisiae* CDC24 and CDC42. *Yeast* *10*, 463–474.